Protein Science (1996), *5*:653–662. Cambridge University Press. Printed in the USA.

The pH dependence of hydrogen-deuterium exchange in *trp* repressor: The exchange rate of amide protons in proteins reflects tertiary interactions, not only secondary structure

MICHAEL D. FINUCANE[1] AND OLEG JARDETZKY
Stanford Magnetic Resonance Laboratory, Stanford University, Stanford, California 94305-5055

(RECEIVED October 23, 1995; ACCEPTED January 29, 1996)

Abstract

The pH dependence of amide proton exchange rates have been measured for *trp*-repressor. One class of protons exchanges too fast to be measured in these experiments. Among the protons that have measurable hydrogen-deuterium exchange rates, two additional classes may be distinguished. The second class of protons are in elements of secondary structure that are mostly on the surface of the protein, and exchange linearly with increasing base concentration (log k_{ex} versus pH). The third class of amide protons is characterized by much higher protection against exchange at higher pH. These protons are located in the core of the protein, in helices B and C. The exchange rate in the core region does not increase linearly with pH, but rather goes through a minimum around pH 6.

The mechanism of exchange for the slowly exchanging core protons is interpreted in terms of the two-process model of Hilton and Woodward (1979, *Biochemistry 18*:5834–5841), i.e., exchange through both a local mechanism that does not require unfolding of the protein, and a mechanism involving global unfolding of the protein. The increase in exchange rates at low pH is attributed to a partial unfolding of the repressor. It is concluded that the formation of secondary structure alone is insufficient to account for the high protection factors seen in the core of native proteins at higher pH, and that tertiary interactions are essential to stabilize the structure.

Keywords: acid denaturation; amide proton hydrogen exchange; local unfolding; nuclear magnetic resonance; proteins

Proteins are tightly packed molecules and, for amide proton exchange to occur from the native state, the structure must be flexible (Linderstrøm-Lang, 1955). For many years now, the nature of the flexibility required has been in dispute. Englander and coworkers (Englander, 1975; Englander et al., 1980; Englander & Mayne, 1992) have proposed a "local unfolding" model in which helices cooperatively unfold to allow exchange to occur in bulk solvent. As an alternative, Woodward and Hilton (1980) have proposed a model in which solvent penetrates the protein matrix, that is, amide protons exchange without any large-scale disruption of secondary structure. The exchange from the native state has a low energy of activation (~20 kcal/mol) and is distinct from the acceleration of amide proton exchange that occurs due to protein unfolding under conditions where the native state is unstable. An excellent review of the distinctions between local and global unfolding, between local unfolding and solvent penetration models, and of the role of hydrogen bonding in protection from exchange has been published recently (Miller & Dill, 1995).

The rate acceleration caused by unfolding of the tertiary structure has been included explicitly as a competitive mechanism to the exchange from the native state by Woodward and coworkers, who have used this combined, "two-process" model to explain the pH and temperature dependence of amide proton exchange in BPTI (Hilton & Woodward, 1979).

The *trp* repressor from *Escherichia coli* is a particularly interesting object for the study of proton exchange because its structure and dynamics are heterogeneous. The repressor is a dimeric protein that regulates the production of tryptophan in the cell. Each monomer consists of six α-helices that are interwoven in the dimer (Fig. 1; Kinemage 1). Helices A, B, C, and F form a tightly packed core region, with helices D and E (which largely form the DNA-binding region) attached as a more loosely bound domain on the surface of the protein (Schevitz et al., 1985; Ar-

Reprint requests to: Oleg Jardetzky, Stanford Magnetic Resonance Laboratory, Stanford University, Stanford, California 94305-5055; e-mail: jardetzky@camis.stanford.edu.

[1] Present address: Department of Biochemistry, University of Sussex, United Kingdom.

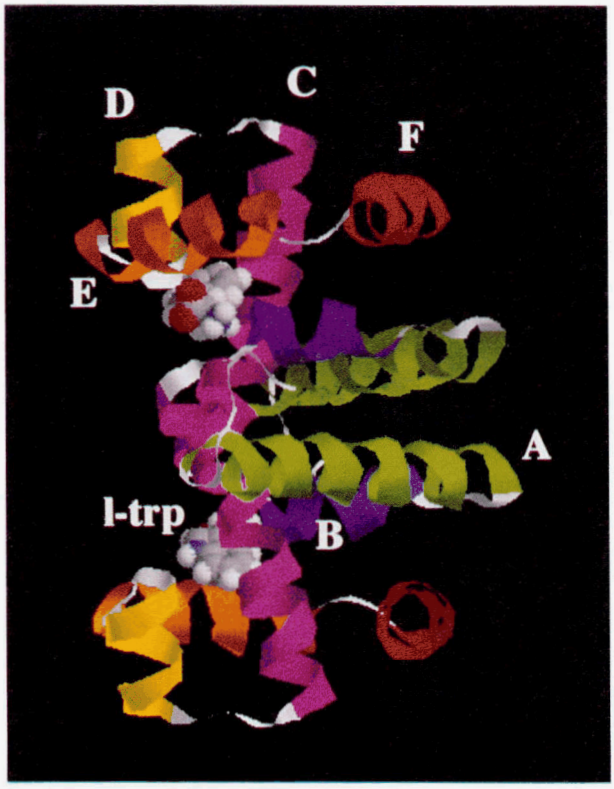

Fig. 1. Ribbon diagram of *trp* repressor taken from the structure of Schevitz et al. (1985). The helices are colored as follows: **(A)** light green; **(B)** purple; **(C)** magenta; **(D)** yellow; **(E)** orange; **(F)** light red. The ligand L-tryptophan is shown in space-filling format, with the ammonium group (nitrogen atom is blue) pointing toward the carbonyl end of helix B.

rowsmith et al., 1991b; Zhao et al., 1993). The DE region was initially identified as being more flexible than the ABCF core on the basis of proton-deuterium exchange (Arrowsmith et al., 1991a; Czaplicki et al., 1991) and proton relaxation measurements (Gryk et al., 1995). This flexibility precludes measurement of exchange rates in the DE region by deuterium exchange, but the rates have been measured by relaxation methods (Gryk et al., 1995; Zheng et al., 1995).

In this study, the exchange rates of the 41 most slowly exchanging residues of *trp*-repressor have been measured as a function of pH. The residues can be considered in two groups on the basis of their exchange rates and the pH dependence of those rates. The exchange rates of the amide protons exchanging more rapidly at pH 7.2 increase linearly with increasing hydroxide concentration, whereas the exchange rates of the protons exchanging more slowly at pH 7.2 first decrease with pH, but as the pH is decreased below about pH 6, increase again. Model amides generally have a minimum in their exchange rates at around pH 3–4, with increasing base catalysis or increasing acid catalysis on either side of this minimum.

These results are consistent with the two-process model of Woodward, which provides the conceptually simplest explanation. They are not consistent with the local unfolding model, which requires correlated exchange of adjacent protons. It must always be remembered, however, that kinetic data can only rule out, but can never prove, specific kinetic models, and that a multiplicity of models can be invoked to account for a given set of data—including modifications of models ruled out in their simplest form. A comprehensive discussion of all models that have been invoked in the analysis of exchange data on proteins is beyond the scope of this report. Our aim is to point out that there are a few conclusions that necessarily follow from the data, whereas specific models do not. To make a definitive choice between specific models—including the widely used Linderstrøm-Lang model and its EX_1/EX_2 formalism—would require additional knowledge that does not exist at this time. The presence and function of a core of more slowly exchanging protons is discussed in relation to the concept of a "folding core" (Kim et al., 1993; Woodward, 1993) and in relation to the requirements for packing elements of secondary structure to form tertiary structure. The implications of the results for studies on protein structure and folding using hydrogen-deuterium exchange methods are also pointed out.

Results

The ^1H-^{15}N HMQC spectrum of *trp*-repressor in ^1H_2O at pH 7.2 is shown in Figure 2A. Representative spectra at pH 7.2 and 5.4 at specified intervals after the fully protonated protein has been dissolved in ^2H_2O are shown in Figure 2B, C, and D. After dissolving the protein in ^2H_2O, only 41 amide protons were distinguishable at any pH between 5.4 and 7.2. The remaining 63 protons (there are 108 residues per monomer, of which 4 are prolines) exchanged too fast for rates to be determined, even at pH 5.4. These amide protons are located in the N-terminal region, in the turns between helices, at the beginning of helices, in the DNA-binding region (helices D and E), and at the carboxy terminus. The exchange rates of these most rapidly exchanging amide protons have been measured by a combination of saturation transfer and inversion recovery methods, and are discussed elsewhere (Gryk et al., 1995; Zheng et al., 1995).

Amide protons that remain in the first spectrum measured after dissolution in ^2H_2O exchange with rate constants of between about 10^{-6} and 10^{-3} s^{-1}. The rates have been measured by fitting the decay in intensity of the ^1H-^{15}N HMQC cross-peaks with time to Equation 1, as described in the Materials and methods. Examples of the decay curves are presented in Figures 3 and 4, showing the quality of the data obtained. Exchange rates reported for pH 5.7 were taken from the study of Czaplicki et al. (1991), and the exchange profiles are not reproduced here.

At pH 7.2, exchange occurs rapidly throughout the repressor (Fig. 2A,B,C). After 2.5 h, most of the amide protons have exchanged with deuterons (Fig. 2B), and the spectrum shows only 15 peaks, one of which (62) is probably overlapped with another peak (26). These peaks are found by reference to the structure to originate in helices A (23, 26, 29); B (38, 40, 41, 42, 43); and C (48, 51, 54, 55, 57, 58, 59, 61, and 62). After 23 h, only residues from the B-C region can be observed (residues 38, 41, 42, 43, 48, 51, 55, 58, and 62; Fig. 2C). Thus, at pH 7.2, the amide protons most resistant to exchange are located, without exception, in helices B and C. This is a region of the protein in which the two monomers interlock to the greatest extent, and that is probably critical for the stability of the dimer. The presence of slowly exchanging amide protons in helix C can be rationalized in terms of C being the least exposed of the helices in the protein. It is packed between helices A, B, E, and F of its own mono-

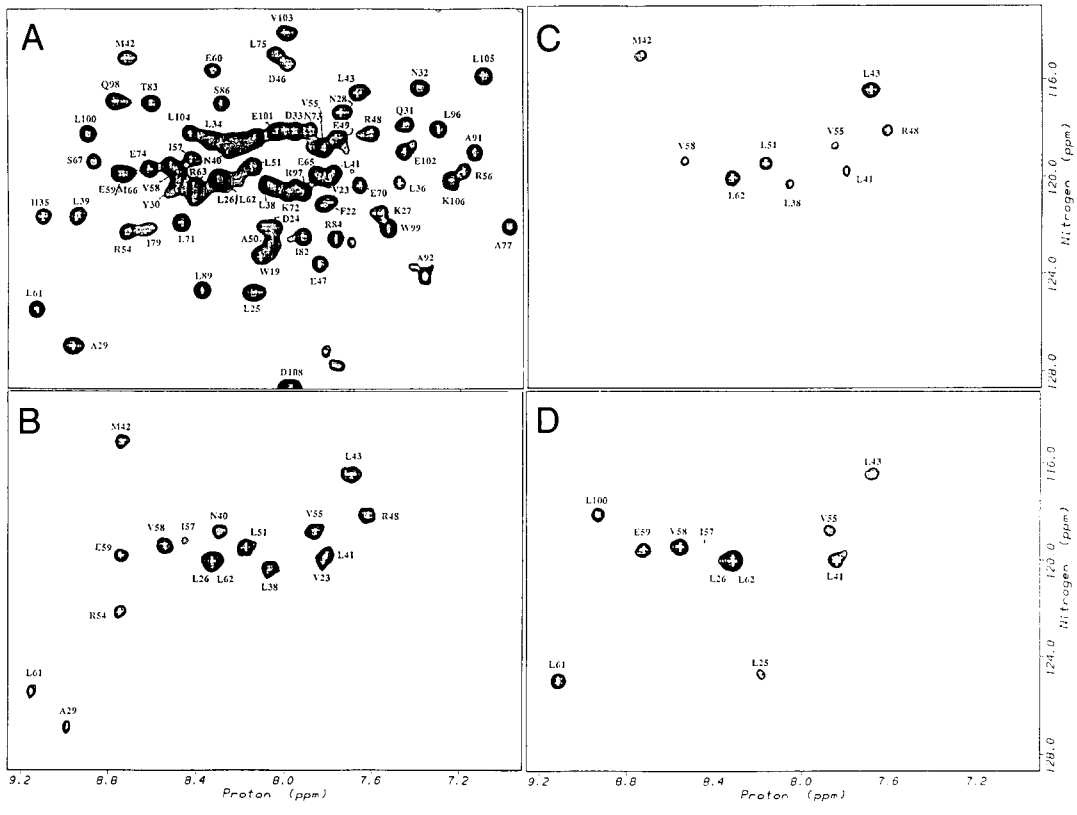

Fig. 2. ^{1}H-^{15}N HMQC spectra of *trp* repressor. Amide protons of the five glycine residues and T44 and E95 resonate outside the region shown in the figure. **A:** Spectrum of the repressor in $^{1}H_2O$ at pH 7.2. **B:** Spectrum at pH 7.2, 2.5 h after dissolution in $^{2}H_2O$. **C:** Spectrum at pH 7.2, 23 h after dissolution in $^{2}H_2O$. **D:** Spectrum at pH 5.4, 90 h after dissolution in $^{2}H_2O$. Samples contained 500 mM NaCl, 50 mM NaH_2PO_4.

mer, and also A, B, E, and F from the other subunit (Fig. 1). Helix B lies near the surface, but differs from the other helices in the protein by having a high proportion of leucine residues (four of eight residues, with an additional leucine at each end of the helix). The carboxyl end of the helix and the turn (L41 and L43) are capped by the alpha-ammonium group of the ligand (Zhang et al., 1987; Fig. 1).

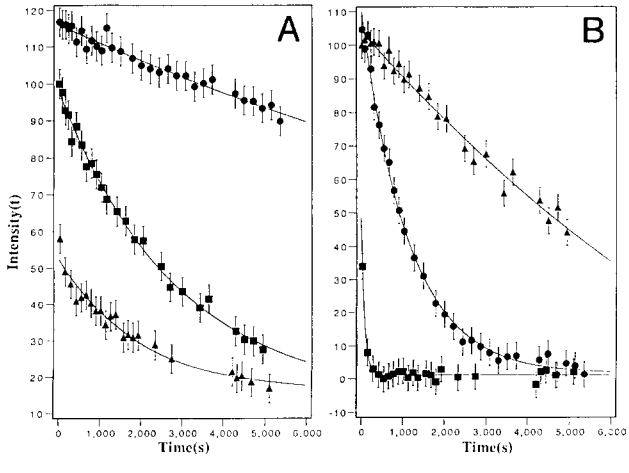

Fig. 3. Decrease in resonance intensity of the amide protons of **(A)** L43 and **(B)** L100 with time after dissolution of the fully protonated repressor in $^{2}H_2O$ at (■) pH 7.2; (●) pH 6.3; and (▲) pH 5.4.

At pH 5.4, a different subset of residues are the last to exchange, i.e., residues 25, (26), 41, 43, 55, 57, 58, 59, 61, 62, 100 (Fig. 2D). At this pH, protons in helices A and F exchange more slowly than protons in helices B and C, which at higher pH are the slowest to exchange. Specifically, residues 25, (26), and 100 exchange more slowly at pH 5.4 than residues 38, 42, 48, 51, and 54, in contrast to the results obtained at pH 7.2, where the opposite is the case. The reason for this becomes apparent when the pH dependence of each residue is examined more closely: residues in helices A and F exchange more slowly as the pH is decreased, in a more or less linear fashion, as may be expected from studies of small peptides (Molday et al., 1972; Bai et al., 1993). This can be seen in Figure 3, for Leu 100. However, amide protons in helices B and C, after initially decreasing in exchange rate with pH, go through a minimum in their exchange curves at around pH 6, and then start to increase their exchange rates with decreasing pH. An example of this is also shown (Leu 43, Fig. 3). This behavior is not expected from studies with model amides, which generally go through a minimum at about pH 3–4 (Molday et al., 1972).

At pH 5.4, the exchange rates of the most slowly exchanging amide protons (41, 42, 43) are similar to each other (Fig. 4). Residues in the first seven hydrogen bonded residues of helix C also

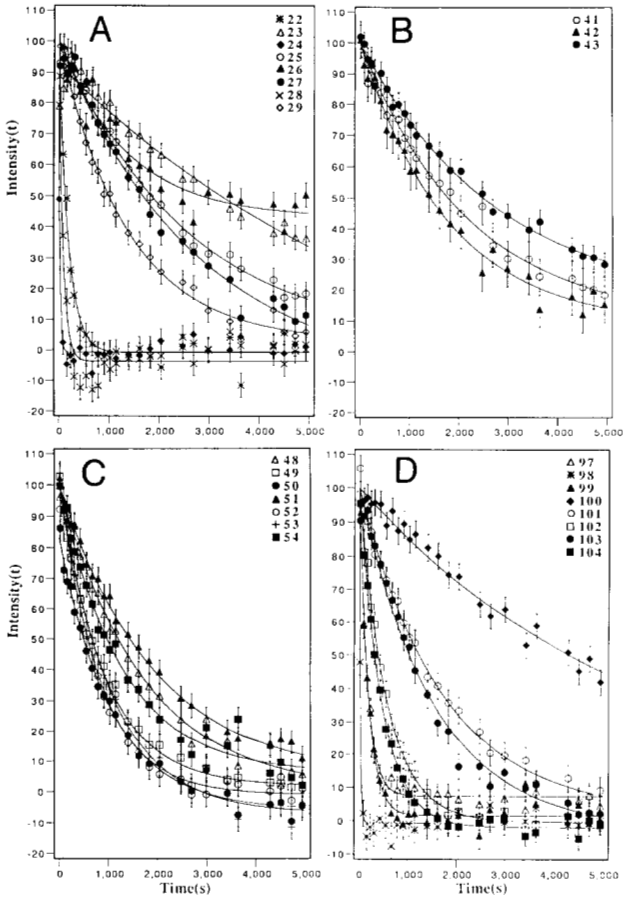

Fig. 4. Decrease in resonance intensity of the amide protons of **(A)** residues 22–29, **(B)** residues 41–43, **(C)** residues 48–54, and **(D)** residues 97–104 with time after dissolution of the fully protonated repressor in ^2H_2O at pH 5.4.

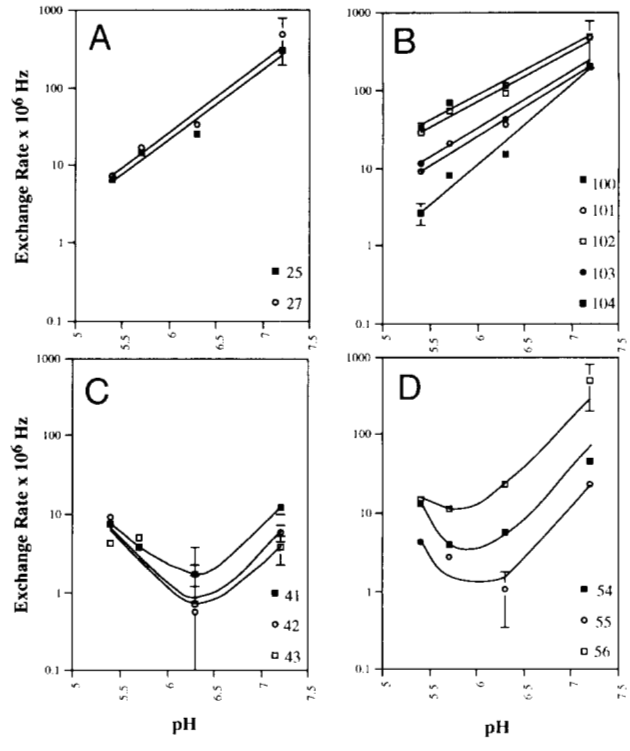

Fig. 5. Dependence of the exchange rate ($\times 10^6$ s^{-1}) on pH for selected residues in **(A)** helix A, **(B)** helix F, **(C)** the B-C turn, and **(D)** helix C.

have similar exchange rates (Fig. 4). This suggests that the exchange is governed by a common opening mechanism. In contrast, amide protons in helices A and F have widely different exchange rates to each other, depending on their location within the helices; amide protons facing the solvent (24 and 28 in A, 98 in F) exchange more rapidly than amide protons facing the interior of the protein (Fig. 4). This suggests that, in contrast to the slower-exchanging set, these amide protons do not exchange by a common opening mechanism. Therefore, the two sets of protons—the more slowly exchanging protons in helices B and C, and the more rapidly exchanging protons in A and F—have different rate-limiting steps governing exchange at low pH.

Different regions of the protein also have different pH dependencies of their amide proton exchange rates. Helices A and F have, in general, a linear correlation of their exchange rates with hydroxide concentration (Fig. 5). Only the pH dependencies of residues L25 and K27 are shown for helix A in Figure 5, because D24 and N28 are too fast to measure at higher pH, whereas L26 is difficult to measure accurately because of overlap with L62. Similarly R97, Q98, and W99 from helix F are not shown in Figure 5 because they exchange rapidly at high pH. Only three examples are shown for helix C, but these cover the range of what is observed. The pH dependence of the exchange rate varies from near linearity (R56) to having a pronounced minimum at pH 6.3 (V55, see Fig. 5). Each of the slowest exchangers—L41, M42, and L43—have a minimum exchange rate at pH 6.3.

The presence of correlated exchange at pH 5.4 is associated with the nonlinearity of the exchange process with hydroxide concentration. Proton exchange rates in regions of the protein that manifest a linear dependence of the exchange rates on pH are uncorrelated with the exchange rates of neighboring protons, as in helices A and F. In contrast, exchange rates of amide protons in B and C, which have minima around pH 6 in their pH dependence, are similar to the exchange rates of neighboring protons. The amide protons of residues 41, 42, and 43 have slightly slower exchange rates at pH 5.4 than the amide protons of residues 48–54 (Fig. 4), and appear to have a slightly higher pH minimum (Fig. 5), which suggests that these two regions may not behave as a single unit, but respond to slightly different mechanisms.

Discussion

The results presented in this paper clearly show the amide protons to be divided into three classes. The first class of protons exchanges too fast to be observable in deuterium exchange experiments. These rates have been measured by proton relaxation methods and are only protected from exchange by approximately one order of magnitude or less (Gryk et al., 1995). The remaining two classes have exchange rates that are measurable by deuterium exchange techniques, and are the subject of the present study. These two classes may be distinguished on the basis of (1) their exchange rates at pH 7.2, (2) correlation of their

exchange rates with those of their neighbors, and (3) the existence of a minimum in their exchange rates between pH 5.4 and 7.2. The protons that exchange more rapidly at pH 7.2 have exchange rates that increase linearly with increasing hydroxide concentration and are not correlated with the exchange rates of their neighbors. These protons are located in helices A and F. The amide protons exchanging more slowly at pH 7.2 show exchange rates that are correlated with those of their neighbors and have minima in their pH profiles between pH 5.4 and 7.2. These protons are located in helices B and C.

Before attempting to understand these different findings and their implications for specific models of exchange, we should note that, quite generally, exchange from a single state is adequate to explain single exponential exchange data and the observed linear increase in exchange rate with base concentration. Two-step models, such as the general Linderstrøm-Lang model or the specific cooperative "local unfolding" model, are *never required* by the usual single-exponential data, although the model may be *compatible with* the data. A two-process model represents a minimum required for interpretation (1) in the more general case, where biexponential exchange behavior is seen (Gryk et al., 1995; Zheng et al., 1995) or (2) when the exchange rate does not show a linear increase with pH, but goes through a minimum in a pH range in which the intrinsic exchange rate of free peptides is a linear function of pH − as in the case presented here.

Also quite generally, without reference to any model, it is possible to define a protection factor as the ratio of the intrinsic rates in free peptides to the observed rate,[2] i.e.,

$$P = \frac{k_i}{k_{obs}}.$$

For a two-step model, P must be regarded as a product of the two protection factors for each of the individual steps, $P = P_A P_B$ (Finucane & Jardetzky, 1995), although the individual factors are only distinguishable when biexponential behavior is observed.

Finally, when identical protection factors are observed for several backbone protons along a polypeptide segment, the exchange can be said to be correlated and it is probable that it involves a cooperative process. Roder et al. (1985a, 1985b) have devised an elegant method for the detection of correlated exchange and have interpreted their results for BPTI in terms of an EX_1 mechanism (Hvidt & Nielson, 1966). This interpretation is consistent with their data, but, as noted above, it requires the additional *assumption* that a two-step model applies and this assumption is not required by the data. Exchange from equally accessible single states of neighboring protons is a possible alternative.

Exchange from helices A and F

The more rapidly exchanging protons have exchange rates that can be described by a single exponential and increase linearly with hydroxide concentration. This behavior has been interpreted in terms of the local unfolding model as EX_2 behavior (Hvidt & Nielsen, 1966; Englander & Mayne, 1992), in which the protection from exchange is defined by the equilibrium constant for local unfolding. However, as noted above, no such local unfolding is required to explain exchange behavior of this type.

The mechanism for exchange from these surface helices cannot be local unfolding, because the amide protons differ widely in their exchange rates (Fig. 4) and protection factors (Fig. 6A), depending on whether they are on the solvent-exposed side of the helix, or on the side facing the interior. For example, the amide protons of D24 and N28 in helix A and Q98 in helix F are all on the solvent-exposed side of the helix, and exchange more rapidly than interior protons. The protection factors do not increase monotonically toward the ends of helices as described for the fraying of isolated peptides.[3] The lack of similar protection factors within regions shows clearly that these helices do not unfold as a unit, but rather respond to individual rate-determining processes.

It is possible that this is generally true for proteins, because, to date, no conclusive evidence has been found for a rate-determining opening of secondary structure associated with the breakage of hydrogen bonds, as predicted by the local unfolding model.[4] This fact has been noted previously by Tuchsen and Woodward (1987). More rapid exchange of the protons on the solvent-exposed face of an helix has been established in the cur-

[2] The protection factor is properly calculated using a value of k_i corrected for primary sequence effects according to the rules of Bai et al. (1993). The protection factors reported in Figure 6 were calculated on this basis.

[3] The increase in the exchange rates for the first three amide protons in any helix is expected regardless of whether fraying occurs or not, because they have no hydrogen bonding partners – only the carbonyl oxygen atoms are hydrogen bonded at the N-terminal ends of helices.

[4] Rate-limiting behavior has been seen at high pH and temperature for BPTI, but only for the slow-exchanging core protons, and has been explained by taking the global unfolding step, not the exchange from the native state, to be rate-limiting (Woodward & Hilton, 1980; see also Roder et al., 1985a, 1985b).

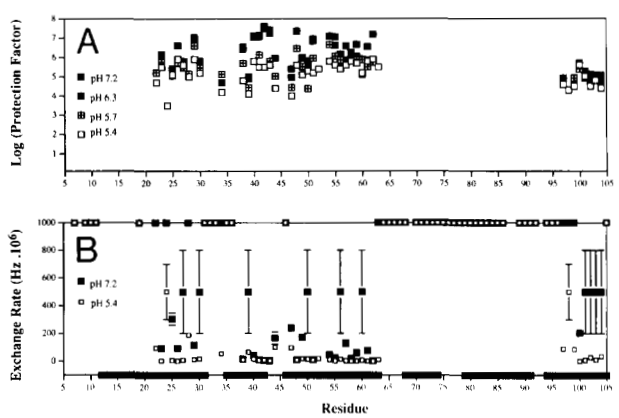

Fig. 6. Variation of the **(A)** logarithm of the protection factor ($k_{intrinsic}/k_{obs}$) and **(B)** the observed exchange rate (k_{obs}) versus residue number in *trp* repressor. Protection factors were calculated using a value of k_i corrected for primary sequence effects according to the rules of Bai et al. (1993). Filled squares along the bottom of graph B indicate the positions of the helices within the X-ray structure (Schevitz et al., 1985). Data points in B at 500×10^6 s^{-1} are rates that are determined for amide protons, which are seen only in the very first spectrum after dissolving the protein in ^2H_2O, and are thus less precise. This fact is reflected by the large error bars.

rent study for *trp* repressor and has been found previously for leucine zipper peptides (Goodman & Kim, 1991), for helix B of Calbindin D_{9k} (Linse et al., 1990), and for helix C of lysozyme (Radford et al., 1992; Pedersen et al., 1993).

Exchange from helices B and C

Mechanism 1

In contrast to the amide protons in the surface helices A and F, there are clearly at least two different mechanisms operating for the more slowly exchanging class of amide protons found in the core. The first mechanism is indistinguishable from the EX_2-like behavior described above; at higher pH, the exchange is linear with pH, and neighboring protons have dissimilar exchange rates, arguing against a cooperative unfolding of helix C as a unit. These rates are, in general, slower than those of surface helices, even at pH 7.2, which is not unexpected because they are more deeply buried in the interior of the protein. At higher pHs, the exchange of the more slowly exchanging amide protons of helices B and C is consistent with the solvent penetration model in the same way as the exchange of the more rapidly exchanging helices A and F.

Mechanism 2

However, at lower pH, the amide protons of helices B and C have exchange rates that increase with decreasing pH. This is not due to increasing acid catalysis, because the pH at which acid catalysis becomes important for amide exchange is much lower, around 3-4 (Molday et al., 1972; Bai et al., 1993). Thus, a second mechanism of decreasing the protection for these amide protons must be operating.

At pH 5.4, the exchange rates for the slowest exchanging protons are similar to each other, approximately 10^{-5} s^{-1} (see Fig. 6B). This rate is greater than that at which the amide protons would exchange at pH 5.4, if the exchange rate had continued to decrease linearly with decreasing hydroxide concentration. Therefore, the protons are becoming accessible in some way to solvent exchange by a more direct route than the local, solvent-penetration type mechanism described above. The simplest model for such increased exchange is that the interior protons are becoming more exposed to solvent, through an unfolding mechanism. The protons are not yet exchanging at the rates expected for fully exposed protons (Bai et al., 1993; Fig. 5A), and so the protein has not yet completely unfolded. This is consistent with the observation of chemical shifts. Proton chemical shifts are reliable indicators of secondary structure within proteins (Jardetzky & Roberts, 1981). Over the pH range 6.0–8.7, the amide proton chemical shifts do not change, and only small (<0.1 ppm) changes occur between pH 5.4 and 6.0. Therefore, the secondary structure remains essentially intact in the pH range 6.0–8.7, and, even at pH 5.4, the amide protons do not adopt random-coil values. Therefore, complete denaturation of the protein has not occurred. Nevertheless, both the increase in the exchange rates for the buried amide protons and the changes in chemical shift indicate that they have become more exposed to solvent. At pH 5.4, the exchange rates for the amide protons in helices B and C are similar to those of helices A and F, and, therefore, the solvent access to the amide protons is probably quite similar in each of the helices at this pH.

At pHs lower than those used in this study, the repressor precipitates. The increase in exchange rate seen at lower pH that we see probably reflects an initial destabilization of the structure. The destabilization with decreasing pH is also apparent from the fact that the protection factors for residues in helices B and C decrease with decreasing pH (Fig. 6A).

It is expected that if the pH were decreased further, so that all of the protein was in the unfolded state, all protons would have similar exchange rates, decreasing linearly with pH. The unfolding at pH 5.4 is not a complete unfolding to a linear peptide with no internal hydrogen bonding or secondary structure. This is evident from the relatively small changes in chemical shift (<0.1 ppm) and by quite large residual protection factors ($<10^{-4}$, Fig. 6A). Rather, it is a process that brings surface and buried helices to a similar exchange rate (Fig. 6B). We propose that the unfolded state observed here, which gives rise to the increased exchange rates for buried protons at pH 5.4, is one in which the tertiary interactions have been disrupted without a corresponding loss in secondary structure content that would be expected to (1) have random-coil chemical shifts and (2) have random-coil exchange rates. In this sense it may resemble the "molten globule" state (Ptitsyn, 1995).

The exchange data by themselves do not distinguish between localized partial unfolding of the tertiary structure and fractional global unfolding (fractions of the molecules undergoing a dimer dissociation in this case). However, the two processes can be distinguished by chemical shift data. In fractional global unfolding, all chemical shifts will change by the same fraction of the shift difference between the folded and unfolded staes, whereas in localized partial unfolding, there will be differential shifts in different parts of the molecule. When the differences are small, as in our case, it is difficult to be absolutely certain of the distinction, but, because we see differential shifts, partial localized unfolding of the tertiary structure appears as the most likely explanation of the exchange data. This is distinct from the local unfolding of secondary structure assumed in the model bearing this name.

The exchange mechanisms occurring at different pH values are summarized in Figure 7. Our hypothesis is that, at low pH, the major contribution to the exchange of the slower-exchanging protons comes from the unfolding of the local tertiary structure, and thus the rates of exchange of these protons are equal ($k_{unfolding}$ is rate-determining). The protons near the surface are exchanging by a penetration/diffusion mechanism that is proceeding without a rate-determining unfolding step, and therefore have variable rates that depend on the accessibility of solvent in the native-state configuration. As the pH increases to pH 7.2, the contribution from the unfolding mechanism to the exchange of the more slowly exchanging amide protons decreases, because the equilibrium constant now favors the folded form, and so the exchange becomes uneven because the penetration/diffusion mechanism becomes the dominant pathway for these protons also.

Location of the slowest exchangers at pH 7.2

The slowly exchanging residues in *trp* repressor are located on the interior faces of the helices, and are highly correlated with hydrophobicity and with the presence of small branched amino acids (valine and leucine). It is notable that helix B, for example, has an abnormally high percentage of leucines and is, by far, the most slowly exchanging surface helix in *trp*-repressor

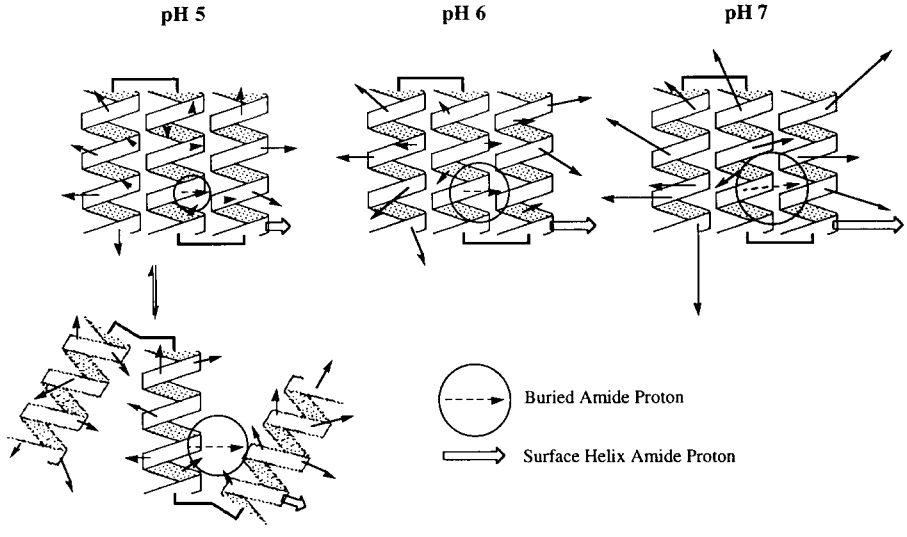

Fig. 7. Two-process model for exchange from *trp* repressor. At pH 5, the repressor partially unfolds, increasing the exchange rates of the most slowly exchanging protons. At this pH, for the most slowly exchanging protons, $k_{obs} \approx k_{unfolding}$. At pH 7, the protein is stable and does not unfold significantly, and the exchange rates depend on the degree of burial of the amide protons from solvent. Arrows represent the exchange of amide protons, with the length of the arrows approximately representing the logarithm of the exchange rates. Dashed arrow represents a typical surface-helix amide proton, and shows the approximately linear increase in $\log(k_{obs})$ with pH. Large arrow represents a typical buried amide proton exchanging, and first decreases in k_{obs}, before increasing, with respect to pH.

at pH 7.2. Slow-exchanging amides are also located in helix C at pH 7.2, but even this nonexposed helix has a greater proportion of fast-exchanging amides than helix B at pH 7.2 (Fig. 6B). Figure 8 shows a stick model of the holorepressor dimer. The location of slow exchangers shown in blue in Figure 8A is very similar to the location of the leucine and valine residues (Fig. 8B, red and green, respectively) within the protein. Within the core region defined by the leucine and valine residues (depicted in space-filling format in Fig. 8C from a "DNA-eye view" and in Kinemage 2), the most slowly exchanging residues (dark blue) are located in the interior, with more peripheral leucine/valine amide protons exchanging less slowly (cyan) and the rapidly exchanging DE helices (white) forming the surface.

Implications of the results for hydrogen exchange in proteins

Our results are consistent with the two-process model proposed by Woodward and coworkers, which postulates the existence of two competitive exchange pathways, an exchange from the native state by solvent penetration and, at low pH, an unfolding pathway in which—as our findings clearly show—the unraveling of the tertiary structure precedes the disintegration of the secondary structure (Hilton & Woodward, 1979; Woodward & Hilton, 1980). They are not consistent with the simple cooperative local unfolding model (Englander et al., 1980).

It has been suggested by Kim et al. (1993) that the slowly exchanging core may be the protein folding core. In support of this suggestion, they quote the fact that in three proteins, the last hydrogens to exchange are in the regions where hydrogens are first protected. This suggestion would lead to the important conclusion that the folding pathway would correspond to regions of the protein arranged in reverse order of their exchange rates, and that this result could be used to determine the folding pathway of proteins (Kim et al., 1993). However, one must be extremely cautious in interpreting pulse-labeling results in this fashion. The method assumes that protons protected by secondary structure do not re-exchange with solvent and the exchanging protons are not protected by secondary structure. This is not necessarily the case. In the *trp*-repressor, it has been demonstrated that there are well-formed helices that exchange rapidly with solvent (Czaplicki et al., 1991; Zhao et al., 1993; Gryk et al., 1995; Zheng et al., 1995; Gryk & Jardetzky, 1996). This has also been demonstrated in the isolated C-terminal proteolytic domain of the *E. coli* tryptophan mark synthase β-chain (Guijarro et al., 1995). If helices such as these are formed first in the folding pathway, they may not show rapid protection as expected, especially at high pH, unless they are buried in the protein interior. The results presented here also demonstrate that amide protons even within well-formed helices (A and F) can exchange rapidly at high pH, where most pulse-labeling exchange is carried out.

The exceptional stability of the more slowly exchanging amide protons in proteins (BPTI, lysozyme, and trypsin and chymotrypsin derivatives) has been attributed to the presence of hydrophobic side chains in the vicinity of an array of hydrogen bonds (Lumry & Gregory, 1986). Although in part the slower exchange rates in the vicinity of hydrophobic side chains may be attributed to their effects on intrinsic exchange rates (Bai et al., 1993), the very large protection factors seen in hydrophobic regions cannot be. It has been suggested that the hydrophobic groups lower the local dielectric constant around the hydrogen bonds, which increases their strength, leading to a decrease in local mobility, and a tightening of the hydrogen bonded network, until the repulsive limit for atom-atom interaction is approached. The correlation of the slowest exchangers with their

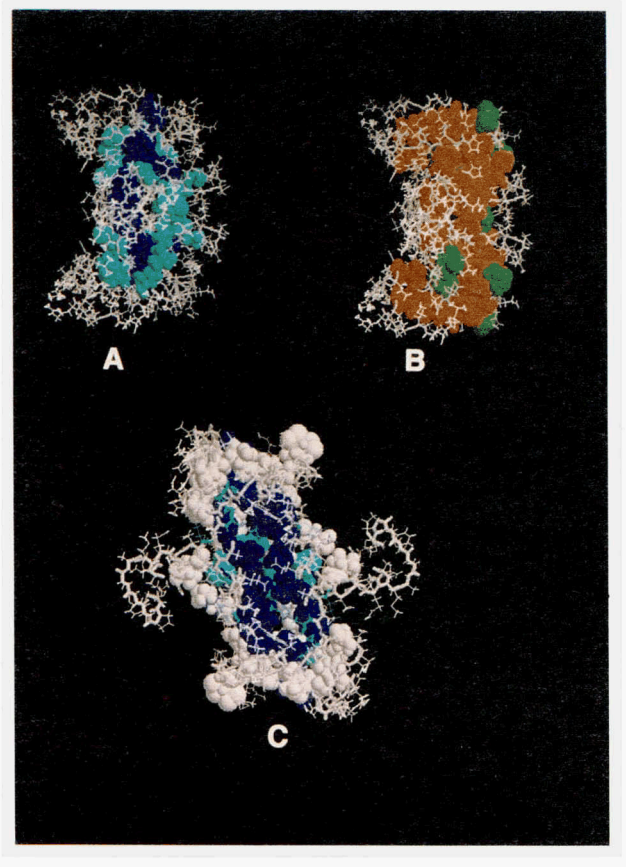

Fig. 8. Models of *trp* repressor generated using Rasmol.[5] **A:** Location of the slowly exchanging amide protons at pH 7.2. Amide protons that exchange between 2.5 and 23 h after dissolution of the fully protonated repressor in ^2H_2O, (i.e., these appear in Fig. 2B, but not in Fig. 2C) are shown in cyan, and amide protons that are still present at pH 7.2 after 23 h (i.e., these appear in Fig. 2C) are shown in dark blue. **B:** Location of the leucine (red) and valine (green) residues within the repressor structure. **C:** View of the *trp* repressor as it would be seen from the DNA, with leucine and valine residues shown in space-filling format. The residues are colored by time of out-exchange as described in Figure 8A. The most slowly exchanging residues are on the interior of the core as defined by the presence of the leucine and valine residues.

location in hydrophobic regions in *trp* repressor is in agreement with this hypothesis. As noted before, the slowly exchanging residues are located in the hydrophobic interior, especially within the leucine-rich regions such as helix B. The presence of a proline 37 within the helix may also assist in the formation of the slow-exchanging core by restricting the backbone conformation of the helix, causing it to bend (Barlow & Thornton, 1988) around helix C, bringing the side chains on the concave side into close contact with each other and with helix C. Small branched hydrophobics may be generally important in forming knot regions in proteins, and have been found to be associated with the packing of helices and β-sheets in protein structures (Ghelis & Yon, 1982).

[5] Roger Sayle and Andrew Bissell, "RasMol: A Program for Fast Realistic Rendering of Molecular Structures with Shadows," Proceedings of the 10th Eurographics UK Conference, University of Edinburgh, April 1992 (available via anonymous FTP from ftp.dcs.ed.ac.uk in the directory /pub/rasmol, and ftp.embl-heidelberg.de in the directory /pub/software).

The observation that the presence of secondary structure does not necessarily correlate with protection from hydrogen exchange has been reported for several proteins. In the experiments of Elöve et al. (1992) on protein folding in cytochrome *c*, 44% regained secondary structure is observed by CD after 4 ms, whereas pulsed H-exchange shows only 10–15% after 3 ms. Similar observations are made on isolated subfragments that lack tertiary contacts to drive the folding to completion (Guijarro et al., 1995), and in subdomains of intact native proteins, which are only loosely bound to the core of the molecule (Czaplicki et al., 1991; Arrowsmith et al. 1991a; Gryk et al., 1995). In the last case, addition of tryptophan, which binds between the core and the outer subdomain, thus binding it more firmly by the addition of further tertiary contacts, slows exchange by an order of magnitude (Finucane & Jardetzky, 1995).

Guijarro et al. (1995) addressed the apparent paradox between results from HD exchange and CD by proposing three alternatives: either (1) CD does not reflect hydrogen bonded structures, but merely geometrically helical and sheet-like structure; (2) high pH (~9) during pulse-labeling destroys such protecting secondary structure as a result of a loss of tertiary structure; or (3) hydrogen bonded structures form under folding conditions, but are flickering in and out of conformation, and are unable to resist exchange. We have observed a fourth alternative, that is, that exchange occurs from intact secondary structures at high pH (Finucane & Jardetzky, 1995; Gryk et al., 1995). The exchange rates may be slow relative to random coil peptides, but no unraveling of the secondary structure is required to explain this result. In the cited work, chemical shift and ^{15}N relaxation data have indicated that exchange occurs from intact α-helices, with *intrinsic* exchange rates calculated from the Linderstrøm-Lang model being two orders of magnitude slower than those predicted by the rules of Bai et al. (1993). Guijarro et al. (1995) finished their paper with a question: "Why are secondary structure elements stabilized in [molten globule-like] intermediates as compared to short peptides in aqueous solution?" The answer to this question, from our results, appears to be that the formation of more stable secondary structures requires tertiary interactions.

Materials and methods

Materials

[U-^{15}N] *trp* repressor was isolated from *E. coli* strain CY15070 carrying the pJPR2 plasmid (Paluh & Yanofsky, 1986) as described previously (Gryk et al., 1995).

The protein was transferred to buffer (500 mM NaCl, 50 mM NaH_2PO_4) of the desired pH by repeated concentration and dilution using an Amicon centriprep-10 unit, and concentrated to between 4 and 5 mM monomer. The protein concentration was determined by A_{280} using an extinction coefficient of 1.2 mg^{-1} mL cm^{-1} (Joachimiak et al., 1983). The aporepressor was converted to the holo- form by the addition of a threefold molar excess of L-tryptophan. The samples were then lyophilized and reconstituted in an identical volume of 99.996% ^2H_2O (Cambridge Isotope Laboratories, Woburn, Massachusetts, USA). Samples were prepared at 45 °C and transferred to the magnet that was at 43 ± 1 °C within 5 min. The pH of each sample has not been corrected for the mole fraction of deuterium oxide present. The initial time was taken to be the time at which the ^2H_2O was added to the sample. Shimming and tuning of the

sample generally required ~10 min, so the dead time of the experiment was approximately 15 min.

NMR spectroscopy

^1H-^{15}N HMQC spectra were recorded at 11.74 *T* on a Bruker AM-500. Data were acquired into 1K data points in t_2 (512 real) and into 200 points (all real) in t_1. The spectra were acquired using a spectral width of 6,493.5 S-1 in t_2 and 3012.1 S-1 in t_1, with quadrature detection using time-proportional phase incrementation. Waltz-16 decoupling was used to decouple ^{15}N during the acquisition period. Suppression of the residual water was carried out using jump-return pulses (Plateau & Gueron, 1982).

All spectral processing was done on a Silicon Graphics Iris Indigo workstation, using the FELIX program developed by Hare Research (version 2). The residual ^1H_2O peak was removed by convolution of the signal, then the spectra were zero-filled once in each dimension, apodized using a sine-bell squared window shifted by $\pi/2$, Fourier transformed, and phase and baseline corrected in both dimensions.

Data fitting and error analysis

Data were fitted to a single exponential decay function using a three-parameter fit to the equation:

$$I_{(t)} = I_\infty + I_0 \exp(-\lambda t). \quad (1)$$

The data were fitted using the Davidon-Fletcher-Powell algorithm (quasi-Newton fit) in the shareware program MacCurvefit 1.1 (Kevin Raner Software).

The coefficient uncertainties reported are the square roots of the diagonal elements of the variance-covariance matrix. For amide protons that did not exchange completely before the experiment was finished, and for which the infinity time-point was not well-determined, the decay curve was fitted using a final intensity of zero.

In some instances (residues 23/41, 26/62, 59/66, 90/55), peaks are known to be significantly overlapped in the ^1H-^{15}N HMQC spectrum in H_2O (Fig. 2A). Residues 66 and 90 are located in stretches of rapidly exchanging amide protons, and have been assumed to have exchanged as rapidly as their neighbors in this study. This assumption is supported by single-exponential decay of the remaining intensity, and peak volumes consistent with the presence of only one peak. The double peak assigned to 23/41 (Fig. 1B) decayed biexponentially. The peaks were sufficiently resolved, however, that the individual rates could be assigned by comparing the contributions of the two rates after a biexponential fit to each of the two subpeaks. Residues 26 and 62 were not sufficiently resolved from each other to be able to reliably assign the rates. However, the decay was essentially single exponential, and the volume remained approximately double the intensity of other amide protons that exchanged with similar rate constants (Fig. 2C). We therefore conclude that the exchange rates of the two peaks are approximately identical.

To exclude the possibility that there were two nonexchanging populations, one of which exchanged rapidly with solvent during the experimental dead time, and one of which exchanged as observed in the experiment (which is possible if, e.g., aggregates are formed), the reverse exchange profile was also measured by dissolving completely amide-deuterated repressor in H_2O and recording successive ^1H-^{15}N HMQC as before. The slow-exchanging protons had only weak intensity in the first spectra (data not shown), which confirmed that the titration was reversible and that only one population of protein molecules was being observed. The spectra were, however, much more crowded than the proton out-exchange experiment, because the more rapidly exchanging protons were present (20 N-terminal + 20 D-E helix + 15 turn amide protons were in this category), making measurements of the rates difficult.

References

Arrowsmith CH, Czaplicki J, Iyer SB, Jardetzky O. 1991a. Unusual dynamic features of the *trp* repressor from *E. coli*. *J Am Chem Soc 113*:4020–4022.

Arrowsmith CH, Pachter R, Altman R, Jardetzky O. 1991b. The solution structures of *E. coli trp* repressor and *trp* aporepressor at an intermediate resolution. *Eur J Biochem 202*:53–66.

Bai Y, Milne JS, Mayne L, Englander SW. 1993. Primary strcture effects on peptide group hydrogen exchange. *Proteins Struct Funct Genet 17*: 75–86.

Barlow DJ, Thornton JM. 1988. Helix geometry in proteins. *J Mol Biol 201*: 601–620.

Czaplicki J, Arrowsmith CH, Jardetzky O. 1991. Segmental differences in the stability of the *trp*-repressor peptide backbone. *J Biomol NMR 1*: 349–361.

Elöve G, Chaffotte AF, Roder H, Goldberg ME. 1992. Early steps in cytochrome *c* folding probed by time-resolved circular dichroism and fluorescence spectroscopy. *Biochemistry 31*:6876–6883.

Englander SW. 1975. Measurement of structural free energy changes in hemoglobin by hydrogen exchange methods. *Ann NY Acad Sci 244*:10–27.

Englander SW, Calhoun DB, Englander JJ, Kallenbach RK, Liem H, Malin EL, Mandal C, Rogero JR. 1980. Individual breathing reactions measured in hemoglobin by hydrogen exchange methods. *Biophys J 32*:577–587.

Englander SW, Mayne L. 1992. Protein folding studied using hydrogen exchange labeling and two-dimensional NMR. *Annu Rev Biophys Biomol Struct 21*:243–265.

Finucane MD, Jardetzky O. 1995. Mechanism of hydrogen-deuterium exchange in *trp*-repressor studied by ^1H-^{15}N NMR. *J Mol Biol 253*:576–589.

Ghelis C, Yon J. 1982. *Protein folding*. New York: Academic Press.

Goodman EM, Kim PS. 1991. Periodicity of amide proton exchange rates in a coiled-coil leucine zipper peptide. *Biochemistry 30*:11615–11620.

Gryk MR, Finucane MD, Zheng Z, Jardetzky O. 1995. Solution dynamics of the *trp*-repressor: A study of amide proton exchange by T1 relaxation. *J Mol Biol 246*:618–627

Gryk MR, Jardetzky O. 1996. AV77 hinge mutation stabilizes the helix-turn-helix domain of *trp* repressor. *J Mol Biol 255*:204–214.

Guijarro JI, Jackson M, Chaffotte AF, Delepierre M, Mantsch HH, Goldberg ME. 1995. Protein folding intermediates with rapidly exchangeable amide protons contain authentic hydrogen-bonded secondary structures. *Biochemistry 34*:2998–3008.

Hilton BD, Woodward CK. 1979. On the mechanism of isotope exchange kinetics of single protons in bovine pancreatic trypsin inhibitor. *Biochemistry 18*:5834–5841.

Hvidt A, Nielsen SO. 1966. Hydrogen exchange in proteins. *Adv Prot Chem 21*:287–386.

Jardetzky O, Roberts GCK. 1981. *NMR in molecular biology*. New York: Academic Press.

Joachimiak A, Kelley RL, Gunsalus RP, Yanofsky C, Sigler PB. 1983. Purification and characterization of *trp* aporepressor. *Proc Natl Acad Sci USA 80*:668–672.

Kim KS, Fuchs JA, Woodward CK. 1993. Hydrogen exchange identifies native-state motional domains important in protein folding. *Biochemistry 32*:9600–9608.

Linderstrøm-Lang K. 1955. Deuterium exchange between peptides and water. *Chem Soc Spec Publ 2*:1–20.

Linse S, Teleman O, Drakenberg T. 1990. Ca^{2+} binding to $Calbindin_{9k}$ strongly affects backbone dynamics: Measurements of exchange rates of individual amide protons using ^1H NMR. *Biochemistry 29*:5925–5934.

Lumry R, Gregory R. 1986. Free-energy management in protein reactions: Concepts, complications and compensation. In: Welch GR, ed. *The fluctuating enzyme*. New York: Wiley Interscience. pp 1–190.

Miller DW, Dill KA. 1995. A statistical mechanical model for hydrogen exchange in globular proteins. *Protein Sci 4*:1860–1873.

Molday RS, Englander SW, Kallen RG. 1972. Primary structure effects on peptide group hydrogen exchange. *Biochemistry 11*:150–158.

Paluh JL, Yanofsky C. 1986. High level production and rapid purification of the *E. coli trp* repressor. *Nucleic Acids Res 14*:7851–7860.

Pedersen TG, Thomsen NK, Andersen KV, Madsen JC, Poulsen FM. 1993. Determination of the rate constants k_1 and k_2 of the Linderstrøm-Lang model for protein amide hydrogen exchange. *J Mol Biol 230*:651–660.

Plateau P, Guéron M. 1982. Exchangeable proton NMR without baseline distortion, using new strong-pulse sequences. *J Am Chem Soc 104*:7310–7311.

Ptitsyn OB. 1995. How the molten globule became. *Trends Biochem Sci 20*:376–379.

Radford SE, Buck M, Topping KD, Dobson CM, Evans PA. 1992. Hydrogen exchange in native and denatured states of hen egg-white lysozyme. *Prot Struct Funct Genet 14*:237–248.

Roder H, Wagner G, Wüthrich K. 1985a. Amide proton exchange in proteins by EX_1 kinetics: Studies of the basic pancreatic trypsin inhibitor at variable p^2H and temperature. *Biochemistry 24*:7396–7407.

Roder H, Wagner G, Wüthrich K. 1985b. Individual amide proton exchange rates in thermally unfolded basic pancreatic trypsin inhibitor. *Biochemistry 24*:7407–7411.

Schevitz RW, Otwinowski Z, Joachimiak A, Lawson CL, Sigler PB. 1985. The three-dimensional structure of *trp* repressor. *Nature 317*:782–786.

Tuchsen E, Woodward C. 1987. Hydrogen exchange kinetics of surface peptide amides in BPTI. *J Mol Biol 193*:703–802.

Woodward C. 1993. Is the slow-exchange core the protein folding core? *Trends Biochem Sci 18*:359–360.

Woodward CK, Hilton BD. 1980. Hydrogen isotope exchange kinetics of single protons in bovine pancreatic trypsin inhibitor. *Biophys J 32*:561–575.

Zhang R-G, Joachimiak A, Lawson CL, Schevitz RW, Ofwinowski Z, Sigler PB. 1987. The crystal structure of *trp* aporepressor at 1.8 Å shows how binding tryptophan enhances DNA affinity. *Nature 327*:591–597.

Zhao D, Arrowsmith CH, Jia X, Jardetzky O. 1993. Refined solution structures of the *E. coli trp* holo- and aporepressor. *J Mol Biol 229*:735–746.

Zheng Z, Gryk MR, Finucane MD, Jardetzky O. 1995. Investigation of protein amide proton exchange by ^1H spin-lattice relaxation. *J Mag Reson Ser B 108*:220–234.